Fast Hybrid Silicon Double-Quantum-Dot Qubit

Zhan Shi,[1] C. B. Simmons,[1] J. R. Prance,[1] John King Gamble,[1] Teck Seng Koh,[1] Yun-Pil Shim,[1] Xuedong Hu,[2] D. E. Savage,[1] M. G. Lagally,[1] M. A. Eriksson,[1] Mark Friesen,[1] and S. N. Coppersmith[1]

[1]*Department of Physics, University of Wisconsin-Madison, Madison, Wisconsin 53706, USA*

[2]*Department of Physics, University at Buffalo, SUNY, Buffalo, New York 14260, USA*

(Received 3 November 2011; revised manuscript received 23 December 2011; published 4 April 2012)

We propose a quantum dot qubit architecture that has an attractive combination of speed and fabrication simplicity. It consists of a double quantum dot with one electron in one dot and two electrons in the other. The qubit itself is a set of two states with total spin quantum numbers $S^2 = 3/4$ ($S = 1/2$) and $S_z = -1/2$, with the two different states being singlet and triplet in the doubly occupied dot. Gate operations can be implemented electrically and the qubit is highly tunable, enabling fast implementation of one- and two-qubit gates in a simpler geometry and with fewer operations than in other proposed quantum dot qubit architectures with fast operations. Moreover, the system has potentially long decoherence times. These are all extremely attractive properties for use in quantum information processing devices.

DOI: 10.1103/PhysRevLett.108.140503 PACS numbers: 03.67.Lx, 73.63.Kv, 85.35.Be

Using electrically gated quantum dots in semiconductor heterostructures to make qubits for quantum information processing [1] is attractive because of the potential for excellent manipulability, scalability, and for integration with classical electronics. Tremendous progress towards the development of working electrically gated quantum dot qubits has been made over the past decade, and single-qubit operations have been demonstrated for logical qubits implemented in single [2], double [3], and triple [4] quantum dots in GaAs heterostructures. However, even with sophisticated pulse sequences that lead to coherence times up to 200 μs [5], the important figure of merit, the number of gate operations that can be performed within the qubit coherence time [6–8], needs to be improved significantly for quantum dot qubits to become useful. Moreover, it is highly desirable that a given implementation be as simple as possible.

In this Letter, we present a relatively simple double-dot qubit architecture in which a universal set of fast gate operations can be implemented. Each qubit consists of a double quantum dot with two electrons in one dot and one electron in the other. The qubit itself is the set of two low-lying electronic states with total spin quantum numbers $S = 1/2$ (square of the total spin of $3\hbar^2/4$) and $S_z = -1/2$ (z component of total spin of $-\hbar/2$). These states form a decoherence-free subspace that is insensitive to long-wavelength magnetic flux noise; moreover, decoherence processes that do not explicitly couple to spin or induce a transition of an electron to the reservoir do not induce transitions that go outside of the subspace of an individual qubit [9]. The gate operations are all implemented using purely electrical manipulations, enabling much faster gates than using ac magnetic fields [1,2], inhomogeneous dc magnetic fields [3,5,10], or mechanisms using spin-orbit coupling [11,12]. The qubit has the same symmetries in spin space as the triple-dot qubit proposed by DiVincenzo *et al.* [13], but is simpler to fabricate because it requires a double dot instead of a triple dot. The hybrid qubit proposed here also has significant advantages over the three-dot qubit for implementing multiqubit operations: two hybrid qubits made of four dots in a linear array have higher effective connectivity than the similar linear array of dots considered in Ref. [13]. We show that this increased effective connectivity can reduce the number of manipulations required to implement two-qubit gates.

We present evidence that implementing this qubit in silicon is feasible. The development of silicon qubits has attracted substantial interest [14–17] because spins in silicon have longer coherence times than spins in many other semiconductors, because of both the weak spin-orbit coupling and the low nuclear spin density in silicon [18–20]. Here, we measure a triplet-singlet relaxation time in a single silicon dot to be >100 ms and demonstrate readout of the singlet and triplet states of two electrons in a silicon dot. We estimate dephasing times theoretically to be on the order of microseconds, long enough to achieve high fidelity quantum operations.

Qubit design.—An important advantage of the qubit proposed here is that all qubit manipulations can be implemented using electric and not magnetic fields, resulting in fast operations [13]. To understand why electrical manipulation of our qubit is possible, we enumerate the possible transitions between spin states of three electrons that can be induced by spin-conserving manipulations. When three spin-1/2 entities are added, the resulting 8 total spin eigenstates form a quadruplet with $S = 3/2$ and $S_z = 3/2, 1/2, -1/2, -3/2$, and two doublets, each with $S = 1/2$, $S_z = \pm 1/2$, where the square of the total spin is $\hbar^2 S(S+1)$ and the z-component of the total spin is $\hbar S_z$. Only states with the same S and S_z can be coupled by spin-independent terms in the Hamiltonian. We choose to use

the group of two states with $S = 1/2$, $S_z = -1/2$ for the states of the qubit.

As discussed in [13], the two states of the logical qubit with $S = 1/2$ and $S_z = -1/2$ can be written as $|0\rangle_L = |S\rangle|\downarrow\rangle$ and $|1\rangle_L = \sqrt{\frac{1}{3}}|T_0\rangle|\downarrow\rangle - \sqrt{\frac{2}{3}}|T_-\rangle|\uparrow\rangle$. In our case, $|S\rangle$, $|T_0\rangle$, and $|T_-\rangle$ are the singlet $((|\uparrow\downarrow\rangle - |\downarrow\uparrow\rangle)/\sqrt{2})$, T_0 triplet $((|\uparrow\downarrow\rangle + |\downarrow\uparrow\rangle)/\sqrt{2})$, and T_- triplet $(|\downarrow\downarrow\rangle)$ in the left dot, and $|\uparrow\rangle$ and $|\downarrow\rangle$ respectively denote a spin-up and spin-down electron in the right dot. The essential difference between our system and that of [13] is that the singlet and triplet states are of two electrons in one dot instead of two different dots, as depicted in Fig. 1.

Single-qubit gate operations.—We now discuss how gate operations are implemented in this qubit in terms of the elementary operations implemented by changes of gate voltages in the device. A complete set of single-qubit manipulations consists of one that changes the energy splitting between the qubit states and another that drives transitions between the qubit states. The energy difference between the two-qubit states is mainly the singlet-triplet splitting in the doubly occupied dot, and this splitting indeed can be tuned by changing gate voltages in both GaAs/GaAlAs [21] and in Si/SiGe dots [22]. In Si/SiGe systems, changing the voltage on a global top-gate should also change the singlet-triplet splitting [23,24].

Transitions between the two states of the hybrid qubit can be induced by changing the off-diagonal terms in the reduced Hamiltonian. These terms are each proportional to $t_i^2/\Delta E_i$, where t_i is the relevant tunneling amplitude and ΔE_i is the energy difference between the relevant state with two electrons on the left dot and the virtual state in which an electron has tunneled from state i in the left dot onto the right dot. Explicit calculations of the effective spin Hamiltonian obtained by a canonical transformation that systematically eliminates higher energy states [25–27] demonstrate that increasing the tunnel couplings between the quantum dots indeed drives transitions between the two states of the qubit (see [28]). Therefore, gate modulations that change the t_i will induce transitions between the qubit states, and modulations of the energy difference ΔE_i will similarly induce transitions when the t_i are non-negligible. We note that when the singlet-triplet splitting Δ_{ST} is non-zero, Rabi flops are performed by modulating the off-diagonal terms at the angular frequency Ω satisfying $\hbar\Omega = \Delta_{ST}$. This modulation is easier to achieve experimentally when Δ_{ST} is not too large. A singlet-triplet splitting of 0.05 meV, typical of splittings measured in quantum dots fabricated in Si/SiGe heterostructures [29,30], corresponds to a frequency of $\sim$10 GHz. Quantum dot gate operations have already been achieved at this speed [31], and efficient schemes exist for refocusing the fast rotations [32].

While the two manipulations obtained by changing the singlet-triplet splitting in one dot or the tunnel coupling between two dots described above are sufficient for achieving arbitrary single-qubit gates, a larger set of elementary operations (or, equivalently, more fine-grained control of the terms in the effective Hamiltonian) is useful because it enables two-qubit gates to be implemented with fewer elementary operations. We note that t_S and t_T, the tunneling matrix elements that shift a single electron from the singlet or triplet state in the left dot to the lowest energy state in the right dot, can be tuned separately. Decreasing the tunnel barrier, as shown in Fig. 1(c), increases both

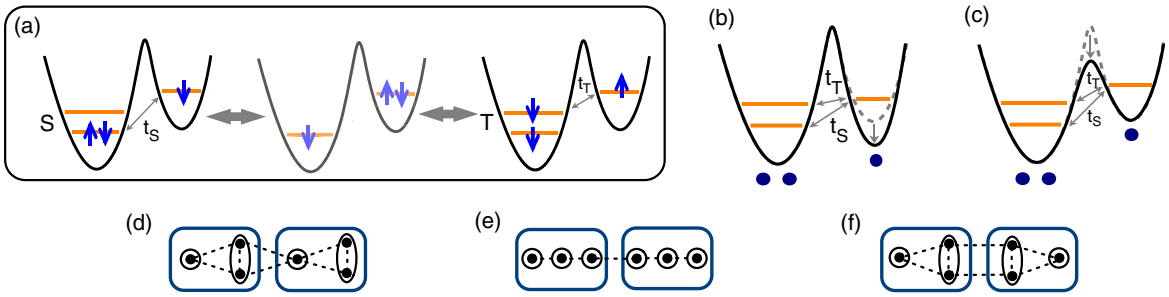

FIG. 1 (color online). The logical qubit states of the hybrid qubit are $|0\rangle_L = |S\rangle|\downarrow\rangle$ and $|1\rangle_L = \sqrt{\frac{1}{3}}|T_0\rangle|\downarrow\rangle - \sqrt{\frac{2}{3}}|T_-\rangle|\uparrow\rangle$, where $|S\rangle$, $|T_-\rangle$, and $|T_0\rangle$ are two-particle singlet (S) and triplet (T) states in the left dot, and $|\uparrow\rangle$ and $|\downarrow\rangle$ respectively denote a spin-up and spin-down electron in the right dot. Fast qubit gate operations are performed by applying gate voltages that change the energy splittings between the singlet and triplet states in the left dot and that change the tunnel couplings t_S and t_T between the two dots. (a): Introducing tunneling between the dots induces transitions between $|0\rangle_L$ and $|1\rangle_L$. Starting from $|0\rangle_L$, in which the electrons in the left dot are in a singlet, if an electron tunnels from the left dot to the right dot, and then the other electron tunnels back to the left dot, the spins in the left dot will end up in a triplet. The actual process conserves the total S^2 and S_z and yields transitions between $|0\rangle_L$ and $|1\rangle_L$ (see [28]). (b) and (c): Schematic illustrating independent tuning of the coupling between the electron in the singly occupied dot and the singlet and triplet states in the doubly occupied dot via the barrier height and relative energies in the two dots, as described in the text. (d): Effective connectivity of two hybrid qubits composed of four dots in a linear geometry. Each connection is a tunable two-electron interaction. There are eight effective connections, compared to five effective connections in a linear array of six dots for the qubits considered in Ref. [13], shown in (e). For (d), a two-qubit gate equivalent to CNOT up to local (one-qubit) unitary operations can be implemented in 16 steps, compared to 18 for (e) [35] (see [28]). (f): Connectivity for which a 14-operation two-qubit gate equivalent to CNOT up to local unitary operations has been found (see [28]).

tunnel rates, whereas changing the difference between the overall energies in the left and right dots, as in Fig. 1(b), can change the ratio of the two tunnel rates, because of energy-dependent tunneling [33,34]. The tunable degrees of freedom (the singlet-triplet splitting and the tunnel rates into the singlet and into the triplet) are denoted schematically in Fig. 1(d) as dashed lines.

Two-qubit gates.—The spin symmetries of the hybrid qubit are the same as in the three-dot qubit of [13] and two-qubit gates are implemented similarly; however, because the hybrid qubit has higher effective connectivity, two-qubit gates can be implemented with fewer elementary operations. The increased connectivity for dots in a linear array is illustrated schematically in Figs. 1(d)–1(f). Figure 1(d) shows two hybrid qubits with eight effective connections, while Fig. 1(e) shows the five effective connections of two triple-dots in a linear array. Figure 1(f) shows a different arrangement of two double-dots, also with eight effective connections ([28] shows how the hybrid qubit can achieve these connections). We have found sequences, presented in [28], of 16 and 14 two-qubit operations that yield gates equivalent to CNOT up to local unitary operations for Fig. 1(d) and Fig. 1(f), respectively. In comparison, the shortest gate sequence that has been found for Fig. 1(e) has 18 operations [35]. These shorter gate sequences provide strong evidence that increased effective connectivity can enable implementation of gates of two logical qubits with fewer elementary two-qubit operations.

Readout and initialization.—Readout of the qubit state can be performed when the tunnel rates coupling the singlet and triplet states of the doubly occupied dot to the lead are significantly different, so that measuring the time to tunnel out of the dot yields information about the qubit state. Different tunnel rates of singlet and triplet states in a single dot have been demonstrated in GaAs [36], and we now show that these rates can also differ significantly in Si.

Figure 2 shows charge sensing measurements of tunnel rates into and out of a Si/SiGe double quantum dot when the occupation of the left dot is changed between one and two. (All electron numbers refer to the effective electron number; the actual number may include a spin-zero closed shell of electrons in addition to the valence electrons we study here. Details of the measurements are in [28].) A step increase in voltage to gate PL causes an electron to tunnel from the lead into the left dot, changing the dot occupation from one to two. Figure 2(b) shows an average of 300 measurements of the charge sensor current in response to the electron tunneling into the dot for $B = 1$ T (when the two-electron ground state is a singlet) and $B = 3$ T (when the two-electron ground state is the triplet T_-), showing exponential decays corresponding to loading a single electron with tunneling rates $\gamma^S_{\text{load}} = 81$ Hz at 1 T and $\gamma^{T_-}_{\text{load}} = 521$ Hz at 3 T [28]. Figure 2(c) shows analogous measurements of electrons tunneling out of the dot that yield tunnel rates $\gamma^S_{\text{unload}} = 182$ Hz and $\gamma^{T_-}_{\text{unload}} = 645$ Hz. The large difference in tunnel rates between the singlet and triplet states provides a mechanism for readout and initialization.

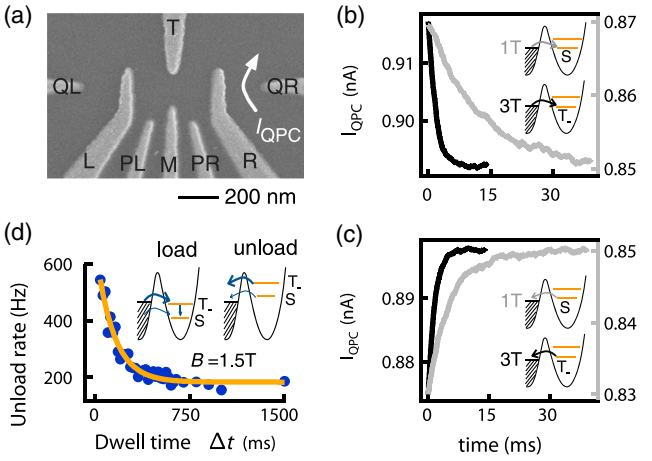

FIG. 2 (color online). Experimental measurements demonstrating readout mechanism (different tunnel rates for the different qubit states) and also a long singlet-triplet relaxation time in a Si/SiGe quantum dot. (a) Scanning electron micrograph of a top-gated Si/SiGe dot with the same gate structure as the one used in the experiment, which is described in [17]. (b) Measurement of the tunnel rates into the dot at 1 T, when the dot ground state is a singlet S (γ^S_{load}, gray line) and at 3 T, when the dot ground state is the triplet T_- ($\gamma^{T_-}_{\text{load}}$, black line). The measured charge sensor current I_{QPC} decreases when the charge in the dot increases, and an exponential fit to I_{QPC} versus time after the voltage on gate PL is changed yields tunnel rates $\gamma^S_{\text{load}} = 81$ Hz and $\gamma^{T_-}_{\text{load}} = 521$ Hz. (c) Analogous measurement of the tunnel rates out of the dot, yielding $\gamma^S_{\text{unload}} = 182$ Hz and $\gamma^{T_-}_{\text{unload}} = 645$ Hz. (d) Measurement of the triplet T_- to singlet S relaxation time T_1, using the method of [36]. The gate voltages on the dot are changed quickly, so both the triplet and singlet states can load, and the unloading rate is measured as a function of the duration of the loading pulse, or dwell time, Δt. As Δt is increased and triplets decay to singlets, the unloading rate decreases. Fitting the unloading rate versus dwell time to an exponential form (shown as the solid line) yields $T_1 = 141 \pm 12$ ms.

Coherence properties.—While the spin symmetries of the hybrid qubit are identical to those of the three-dot qubit in [13], the coherence properties are different because the singlet and triplet states have different spatial wave functions. An essential component of this qubit is a long lifetime for the triplet state of the dot with two electrons. We measure this lifetime by applying a step in voltage to gate PL large enough that both the ground state singlet S and the triplet T_- excited state are energetically accessible at magnetic field $B = 1.5$ T. States S and T_- each load with some probability. After a dwell time Δt, the voltage is returned to its previous value, and an electron tunnels out of the dot. As Δt is increased, the probability that the electrons remain in the T_- state decreases exponentially with a characteristic time T_1, and the tunnel rate to the lead

decays with the same characteristic time. Figure 2(d) shows the result of such a measurement; it yields $T_1 = 141 \pm 12$ ms. This slow relaxation time is significantly longer than the value of ~3 ms measured in GaAs [36] and is consistent with theoretical estimates that account for Rashba spin-orbit coupling and phonon-assisted hyperfine coupling [37,38].

The different charge distributions of the two-qubit states gives rise to dephasing due to electron-phonon coupling [39,40] and charge noise [41]. Our calculations indicate that for realistic states, the intervalley component of the electron-phonon dephasing term is the most important, and leads to $T_2 \sim 1$ μs [42]. Dephasing due to charge noise is suppressed in the hybrid qubit compared to charge qubits [43] because the changes in charge distributions are confined to a single quantum dot, making the effective dipole moment much smaller (indeed, the dipole moment vanishes in the limit of harmonic dot potentials) [42]. Therefore, charge fluctuation-induced decoherence is greatly suppressed in the hybrid qubit compared to double-dot charge qubits. Simple estimates indicate that decoherence rates induced by nuclear spins will be similar to those in singlet-triplet qubits [5].

Summary.—We propose a solid state qubit architecture consisting of three electrons in two quantum dots. Compared to previous proposals, this new qubit has the important advantages of fast gate operations and relative simplicity of fabrication. Experimental data are presented that support the feasibility of constructing the qubit architecture using Si/SiGe quantum dots.

We acknowledge useful conversations with Malcolm Carroll, Robert Joynt, and Charles Tahan. This work was supported in part by ARO and LPS (W911NF-08-1-0482), by NSF (DMR-0805045, PHY-1104660, and a graduate fellowship to J. K. G.), and by United States Department of Defense. The U.S. government requires publication of the following disclaimer: the views and conclusions contained in this document are those of the authors and should not be interpreted as representing the official policies, either expressly or implied, of the U.S. Government. This research utilized NSF-supported shared facilities at the University of Wisconsin-Madison.

[1] D. Loss and D. P. DiVincenzo, Phys. Rev. A **57**, 120 (1998).
[2] F. H. L. Koppens, C. Buizert, K. J. Tielrooij, I. T. Vink, K. C. Nowack, T. Meunier, L. P. Kouwenhoven, and L. M. K. Vandersypen, Nature (London) **442**, 766 (2006).
[3] J. R. Petta, A. C. Johnson, J. M. Taylor, E. A. Laird, A. Yacoby, M. D. Lukin, C. M. Marcus, M. P. Hanson, and A. C. Gossard, Science **309**, 2180 (2005).
[4] E. A. Laird, J. M. Taylor, D. P. DiVincenzo, C. M. Marcus, M. P. Hanson, and A. C. Gossard, Phys. Rev. B **82**, 075403 (2010).
[5] H. Bluhm, S. Foletti, I. Neder, M. Rudner, D. Mahalu, V. Umansky, and A. Yacoby, Nature Phys. **7**, 109 (2010).
[6] D. P. DiVincenzo, Science **270**, 255 (1995).
[7] J. Preskill, Proc. R. Soc. A **454**, 469 (1998).
[8] A. Fisher, Phil. Trans. R. Soc. A **361**, 1441 (2003).
[9] D. A. Lidar, I. L. Chuang, and K. B. Whaley, Phys. Rev. Lett. **81**, 2594 (1998).
[10] J. Levy, Phys. Rev. Lett. **89**, 147902 (2002).
[11] E. I. Rashba, Phys. Rev. B **78**, 195302 (2008).
[12] V. N. Golovach, M. Borhani, and D. Loss, Phys. Rev. B **74**, 165319 (2006).
[13] D. P. DiVincenzo, D. Bacon, J. Kempe, G. Burkard, and K. B. Whaley, Nature (London) **408**, 339 (2000).
[14] B. E. Kane, Nature (London) **393**, 133 (1998).
[15] M. Xiao, M. G. House, and H. W. Jiang, Phys. Rev. Lett. **104**, 096801 (2010).
[16] A. Morello, J. Pla, F. Zwanenburg, K. Chan, K. Tan, H. Huebl, M. Mottonen, C. Nugroho, C. Yang, J. van Donkelaar, A. Alves, D. Jamieson, C. Escott, L. Hollenberg, R. Clark, and A. Dzurak, Nature (London) **467**, 687 (2010).
[17] C. B. Simmons, J. R. Prance, B. J. Van Bael, T. S. Koh, Z. Shi, D. E. Savage, M. G. Lagally, R. Joynt, M. Friesen, S. N. Coppersmith, and M. A. Eriksson, Phys. Rev. Lett. **106**, 156804 (2011).
[18] C. Tahan, M. Friesen, and R. Joynt, Phys. Rev. B **66**, 035314 (2002).
[19] R. de Sousa and S. Das Sarma, Phys. Rev. B **67**, 033301 (2003).
[20] A. M. Tyryshkin, S. Tojo, J. J. L. Morton, H. Riemann, N. V. Abrosimov, P. Becker, H.-J. Pohl, T. Schenkel, M. L. W. Thewalt, K. M. Itoh, and S. A. Lyon, Nature Mater. **11**, 143 (2011).
[21] S. Amasha, K. MacLean, I. P. Radu, D. M. Zumbühl, M. A. Kastner, M. P. Hanson, and A. C. Gossard, Phys. Rev. B **78**, 041306 (2008).
[22] Z. Shi, C. B. Simmons, J. R. Prance, J. K. Gamble, M. Friesen, D. E. Savage, M. G. Lagally, S. N. Coppersmith, and M. A. Eriksson, Appl. Phys. Lett. **99**, 233108 (2011).
[23] T. B. Boykin, G. Klimeck, M. Friesen, S. N. Coppersmith, P. vonAllmen, F. Oyafuso, and S. Lee, Phys. Rev. B **70**, 165325 (2004).
[24] A. L. Saraiva, M. J. Calderon, X. Hu, S. Das Sarma, and B. Koiller, Phys. Rev. B **80**, 081305(R) (2009).
[25] J. R. Schrieer and P. A. Wolff, Phys. Rev. **149**, 491 (1966).
[26] C. Gros, R. Joynt, and T. M. Rice, Phys. Rev. B **36**, 381 (1987).
[27] A. H. MacDonald, S. M. Girvin, and D. Yoshioka, Phys. Rev. B **37**, 9753 (1988).
[28] See Supplemental Material at http://link.aps.org/supplemental/10.1103/PhysRevLett.108.140503 for details of the calculations and experimental procedures.
[29] S. Goswami, K. A. Slinker, M. Friesen, L. M. McGuire, J. L. Truitt, C. Tahan, L. J. Klein, J. O. Chu, P. M. Mooney, D. W. van der Weide, R. Joynt, S. N. Coppersmith, and M. A. Eriksson, Nature Phys. **3**, 41 (2007).
[30] M. G. Borselli, R. S. Ross, A. A. Kiselev, E. T. Croke, K. S. Holabird, P. W. Deelman, L. D. Warren, I. Alvarado-Rodriguez, I. Milosavljevic, F. C. Ku, W. S. Wong,

A. E. Schmitz, M. Sokolich, M. F. Gyure, and A. T. Hunter, Appl. Phys. Lett. **98**, 123118 (2011).
[31] J. R. Petta, A. C. Johnson, C. M. Marcus, M. P. Hanson, and A. C. Gossard, Phys. Rev. Lett. **93**, 186802 (2004).
[32] J. A. Jones and E. Knill, J. Magn. Reson. **141**, 322 (1999).
[33] K. MacLean, S. Amasha, I. P. Radu, D. M. Zumbühl, M. A. Kastner, M. P. Hanson, and A. C. Gossard, Phys. Rev. Lett. **98**, 036802 (2007).
[34] C. B. Simmons, T. S. Koh, N. Shaji, M. Thalakulam, L. J. Klein, H. Qin, H. Luo, D. E. Savage, M. G. Lagally, A. J. Rimberg, R. Joynt, R. Blick, M. Friesen, S. N. Coppersmith, and M. A. Eriksson, Phys. Rev. B **82**, 245312 (2010).
[35] B. H. Fong and S. M. Wandzura, Quantum Inf. Comput. **11**, 1003 (2011).
[36] R. Hanson, L. H. Willems van Beveren, I. T. Vink, J. M. Elzerman, W. J. M. Naber, F. H. L. Koppens, L. P. Kouwenhoven, and L. M. K. Vandersypen, Phys. Rev. Lett. **94**, 196802 (2005).
[37] M. Prada, R. H. Blick, and R. Joynt, Phys. Rev. B **77**, 115438 (2008).
[38] L. Wang and M. W. Wu, J. Appl. Phys. **110**, 043716 (2011).
[39] X. Hu, B. Koiller, and S. Das Sarma, Phys. Rev. B **71**, 235332 (2005).
[40] X. Hu, Phys. Rev. B **83**, 165322 (2011).
[41] D. Culcer, X. Hu, and S. Das Sarma, Appl. Phys. Lett. **95**, 073102 (2009).
[42] J. K. Gamble, M. Friesen, S. N. Coppersmith, and X. Hu, arXiv:1203.6332.
[43] T. Hayashi, T. Fujisawa, H. D. Cheong, Y. H. Jeong, and Y. Hirayama, Phys. Rev. Lett. **91**, 226804 (2003).